

# EVALUATION OF A NONDIFFRACTING TRANSDUCER FOR TISSUE CHARACTERIZATION

Jian-yu Lu and James F. Greenleaf

Biodynamics Research Unit, Department of Physiology and Biophysics,  
Mayo Clinic and Mayo Foundation  
Rochester, MN 55905

## ABSTRACT

Variations in beam width caused by diffraction create difficulties when estimating material properties from ultrasound signals. Tissue characterization will be more easily performed if a beam that does not diverge over large distances can be produced.

In this paper, acoustical backscatter coefficients of scattering objects were estimated using a  $J_0$  Bessel nondiffracting beam that was first introduced by J. Durnin in optics in 1987 and using the data reduction method proposed by Madsen et al. We present a formula for the calculation of backscatter coefficients that requires only two one-dimensional integrations in addition to one-dimensional Fourier transforms (four-dimensional integrations at various transducer-scattering volume distances are required if a conventional circularly symmetric focused transducer is used). This equation in combination with backscatter from a  $J_0$  Bessel nondiffracting beam results in the capability of calculating backscatter coefficients in real time. In addition, estimations of the backscatter coefficients are more distance independent because of the nonspreading nature of the  $J_0$  Bessel nondiffracting beam. Experiments on both excised human liver samples and an RMI413A tissue equivalent phantom were presented and the results were compared to those obtained by a conventional focused Gaussian beam transducer.

## INTRODUCTION

Conventionally, characterizations for tissue acoustic properties are performed with transducers that suffer from beam diffraction. Procedures to overcome beam diffraction are usually very complex and hence computationally inefficient. Estimations of tissue properties would be simplified greatly if a beam that does not diverge over large distances could be produced.

A beam that does not spread was discovered by J. Durnin in 1987 [1] and a  $J_0$  Bessel nondiffracting beam was realized with an optical experiment [2]. Some studies of nondiffracting beams in optics and acoustics have been performed by other investigators [3-11].

We have developed a ten annular element  $J_0$  Bessel ultrasonic nondiffracting transducer and have reported measurements of its continuous and pulsed wave fields in water [12]. Its pulse-echo imaging capability has also been reported [13]. In this paper we report the application of the  $J_0$  Bessel nondiffracting transducer for estimation of backscatter coefficient [14-16]. We adapted the data reduction method proposed by Madsen et al. [14] for the estimation of backscatter coefficients using the  $J_0$  Bessel nondiffracting transducer. Because of the nonspreading nature of the  $J_0$  Bessel nondiffracting transducer, the formula for estimating backscatter coefficients in the data reduction method was greatly simplified resulting in more distance independent estimations of backscatter coefficients. Good agreement between the backscatter coefficients estimated by the  $J_0$  Bessel nondiffracting transducer and the conventional focused Gaussian beam transducer was achieved.

In the METHOD section we present a brief review of the  $J_0$  Bessel nondiffracting beam and a derivation of a formula for calculating the backscatter coefficients using the  $J_0$  Bessel nondiffracting transducer. In the EXPERIMENTS and RESULTS sections we provide experimental methods and results for estimating the backscatter coefficients of excised human liver samples and RMI413A tissue equivalent phantom.

## METHOD

A  $J_0$  Bessel nondiffracting solution to the scalar wave equation was discovered by J. Durnin in 1987 [1] to be:

$$U(\vec{r}, \omega) = J_0(\alpha \rho) e^{j\beta z} \quad (1)$$

where  $U(\vec{r}, \omega)$  is a complex wave field at position  $\vec{r}$  and angular frequency  $\omega$ ,  $J_0(\alpha \rho)$  is zeroth order Bessel function with the first kind,  $\alpha$  is a scaling parameter which determines the width of the central lobe of the  $J_0$  Bessel function,  $Z$  is axial distance away from wave sources,  $\beta$  is related to  $\alpha$  by  $\beta = \sqrt{(\omega/c)^2 - \alpha^2}$  and  $\alpha < \omega/c$ , where  $c$  is speed of sound.

Following the data reduction method proposed by Madsen et al. [14], backscatter coefficients can be estimated by the following equation:

$$\eta(\omega_0) \xrightarrow{\tau \text{ increasing}} \frac{|\tilde{V}_s(\omega_0)|^2}{\left(\frac{\tau}{2\pi}\right)^2 \iiint_{\Omega} d\vec{r}' ||J'_{\omega_0}(\vec{r}')||^2} \quad (2)$$

where  $\eta(\omega_0)$  is the backscatter coefficient calculated at angular frequency  $\omega = \omega_0$ ,  $|\tilde{V}_s(\omega_0)|^2$  is an ensemble average of the modulus square of Fourier transform of backscattered signals calculated at  $\omega_0$ ,  $\tau$  is width of a time gate applied to the backscattered signals,  $\Omega$  defines a scattering volume with which incident wave is interrogated,  $J'_{\omega_0}(\vec{r}')$  is given by:

$$J'_{\omega_0}(\vec{r}') \equiv 2\pi \int_{-\infty}^{\infty} d\omega' T(\omega') B_o^*(\omega') \frac{e^{-j(\omega_0 - \omega')\tau} - 1}{-j(\omega_0 - \omega')\tau} e^{-j(\omega_0 - \omega')t_0} \left[ (j\lambda U(\vec{r}', \omega'))^* \right]^2 \Big|_{t_0 = 2r_p/c} \quad (3)$$

where  $T(\omega)B_o(\omega)$  is a system transfer function of the transducer which includes the spectrum of the electrical excitation pulse, and the transmitting and receiving transfer function of the transducer (it can be obtained experimentally in a way described in the next section),  $\lambda$  is wavelength,  $r_p$  is the nearest distance to scattering volume from the transducer, and \* represents a complex conjugate.

Inserting Eqs. (1) and (3) into Eq. (2), a formula for estimating the backscatter coefficients using the  $J_0$  Bessel nondiffracting transducer is obtained:

$$\eta(\omega_0) \xrightarrow{\tau \text{ increasing}} \frac{|\tilde{V}_s(\omega_0)|^2}{\frac{(2\pi)^7 \tau^2 c^5}{2} \int_0^a J_0^4(\alpha\rho) \rho d\rho \int_0^\tau dt \left| \mathcal{F}^{-1} \left\{ T^*(\omega') B_o^*(\omega') \frac{e^{j(\omega_0 - \omega')\tau} - 1}{(\omega_0 - \omega')\tau} \right\} (t) \right|^2} \quad (4)$$

where  $\mathcal{F}^{-1}$  represents inverse Fourier transform.

For attenuating media having an attenuation coefficient  $\sigma(\omega_0)$  at angular frequency  $\omega_0$ , if  $\omega_0/c - \alpha \gg \sigma(\omega_0)$ , and  $\tau$  is so small that within which the attenuation is negligible, Eq. (4) can be written as:

$$\eta(\omega_0) \xrightarrow{\tau \text{ increasing}} \frac{|\tilde{V}_s(\omega_0)|^2 e^{4\sigma(\omega_0)z}}{\frac{(2\pi)^7 \tau^2 c^5}{2} \int_0^a J_0^4(\alpha\rho) \rho d\rho \int_0^\tau dt \left| \mathcal{F}^{-1} \left\{ T^*(\omega') B_o^*(\omega') \frac{e^{j(\omega_0 - \omega')\tau} - 1}{(\omega_0 - \omega')\tau} \right\} (t) \right|^2} \quad (5)$$

From Eq. (5) it is seen that after compensation for attenuation, B-scan images obtained by the  $J_0$  Bessel nondiffracting transducer with a narrow band tone burst excitation will be related directly to the distributions of the backscatter coefficients. Because of the nonspreading nature of the  $J_0$  Bessel beam, the computation requirements are greatly reduced (two one-dimensional integrations in addition to Fourier transforms, see Eq. (5)) as compared to those when using circularly symmetric focused transducers (four-dimensional integrations for various transducer-scattering volume distances are required, see Eqs. (2) and (3)).

## EXPERIMENTS

Figure 1 shows the experimental system for estimating the backscatter coefficients of scattering objects. A polynomial waveform synthesizer (Model Data 2045) was used to produce 2.5 MHz 5  $\mu$ s tone bursts. The tone bursts were amplified to drive a ten element annular array transducer which could be weighted by either stepwise  $J_0$  Bessel functions or stepwise Gaussian functions along its radius (the differences between the stepwise approximations and exact ones are negligible when  $Z/D > 1$  [13], where  $Z$  and  $D$  are axial distance and diameter of the transducer, respectively). The echoes were amplified, 8 bit A/D converted and gated with a time window of width  $\tau = 10 \mu$ s. The digitized signals (sampling rate was 40 megasamples/second) were stored on disk for signal processing. The system was controlled by a computer which triggered generation of the tone bursts, synchronized scanning of the transducer and data acquisition. Twenty-five A-lines along a 6.25 mm scanning width were collected. Backscatter coefficients were estimated for a region of interest in human liver samples or a RMI413A tissue equivalent phantom placed at  $Z/D = 1.0, 2.0, 3.0$ , and 4.0 (for the  $J_0$  Bessel nondiffracting transducer) or  $Z/D = 1.0, 2.4$  ( $f$ -number), 3.0, and 4.0 (for the focused Gaussian beam transducer).

For calculating the backscatter coefficients, system transfer functions of the transducers must be known. A method suggested by Madsen et al. [14] for determining the system transfer functions of the transducers,  $T(\omega)B_o(\omega)$ , was used. In the method, a planar reflector is used. A water-castor oil interface which has an amplitude reflecting coefficient of 0.0217 at 20°C was chosen as a planar reflector and was placed 50 mm and 120 mm (focal length

of the transducer) away from the  $J_0$  Bessel nondiffracting transducer and the focused Gaussian beam transducer, respectively, for determining the system transfer functions of the transducers.

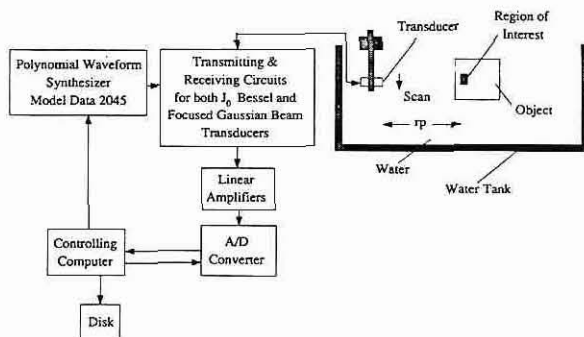


Figure 1 Experimental system for backscatter coefficient measurements.

The human liver samples were obtained from autopsy. They were fixed in 10% formalin fluid for several days and then degassed and sealed into a plexiglass box with dimension of 200 mm (long) x 110 mm (wide) x 130 mm (high). An acoustic window on the top of the box was made of polyester film of thickness of 0.125 mm. Relatively uniform areas in the human liver samples and the RMI413A tissue equivalent phantom were chosen as regions of interest that are 6.25 mm x 7.5 mm in size. The regions of interest were selected as close as possible to the top of the human liver samples and the RMI413A tissue equivalent phantom to reduce initial attenuation of the backscattered signals.

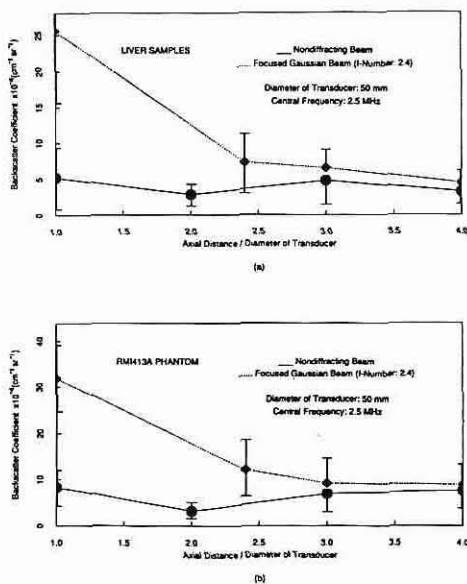


Figure 2 The backscatter coefficients estimated by the  $J_0$  Bessel nondiffracting transducer (solid lines) and the focused Gaussian beam transducer (dashed lines,  $f$ -number = 2.4) at various values of  $Z/D$ , where  $Z$  and  $D$  (50 mm) are the distance and diameter of the transducer, respectively. 5  $\mu$ s 2.5 MHz tone bursts were used for the measurement and a 10  $\mu$ s time window was used to gate the backscattered signals. (a) The backscatter coefficients of the excised human liver samples. (b) The backscatter coefficients of the commercial RMI413A tissue equivalent phantom.

## RESULTS

Figure 2(a) shows the backscatter coefficients of the excised human liver samples measured with the  $J_0$  Bessel nondiffracting transducer (solid lines) and the focused Gaussian beam transducer (dotted lines) when the same region of interest in the excised human liver samples were located at several  $Z/D$  values. Initial attenuation due to the tissue between the region of interest and the top of the liver samples was compensated. The vertical bars represent the standard deviation of the estimated backscatter coefficients. Figure 2(b) is the same as Fig. 2(a), except that the backscatter coefficients of the commercial RMI413A tissue equivalent phantom were estimated. From Fig. 2 it is seen that the backscatter coefficients obtained by the  $J_0$  Bessel nondiffracting transducer are consistent with each other for  $Z/D$  from 1.0 to 4.0 and are very close to those obtained by the focused Gaussian beam transducer for values of  $Z/D > 2.4$  and are in the same range as previously reported results for excised normal human livers [17]. When  $Z/D < 2.4$ , the backscatter coefficients obtained by the focused Gaussian beam transducer increase significantly. This phenomenon was reported by other investigators [16].

## DISCUSSION

There was good agreement between experimental results and theoretical prediction of backscatter coefficients using focused transducers in the data reduction method, except for small  $Z/D$  values [16]. It is seen from Fig. 2 that the backscatter coefficients estimated by the  $J_0$  Bessel nondiffracting transducer are very close to those obtained by the focused Gaussian beam transducer. This suggests a successful implementation of the data reduction method for the  $J_0$  Bessel nondiffracting transducer. In addition, the estimated backscatter coefficients are more distance independent than those obtained by the focused Gaussian beam transducer and the computation requirement is greatly reduced. This demonstrates that the beam of the  $J_0$  Bessel nondiffracting transducer is nonspreading over large depth of field and is a useful tool in tissue characterization.

### Variations and Standard Deviations

Figure 2 shows variations of the backscatter coefficients with distance. These variations are caused by the complexity of scattering objects and are sensitive to the interference of the incident wave with structures of the scattering objects. For the  $J_0$  Bessel nondiffracting transducer, narrow band tone bursts will cause a rough variation of the pulse-echo impulse responses along the central axial axis of the transducer. This variation will also contribute to the variations of the backscatter coefficients with distance.

The standard deviations for the backscatter coefficients measured are quite large. The standard deviations were derived from 25 backscattered signals that were obtained by scanning the transducers in a lateral direction. The large standard deviations mean there are

strong inhomogeneities of the scattering objects in the scanning direction.

### In vivo Measurement of Backscatter Coefficients

It is seen from Eq. (5) that for *in vivo* estimation of the backscatter coefficients with the  $J_0$  Bessel nondiffracting transducer, the estimation should be corrected for the tissue attenuation,  $e^{4\sigma(\omega_0)z}$ . Therefore, estimation of tissue attenuation coefficients  $\sigma(\omega_0)$  which might be a function of  $\vec{r}$ , is very important for a quantitative *in vivo* measurement of backscatter coefficients.

### Imaging of Backscatter Coefficients

It may be more useful for medical diagnosis to perform backscatter coefficient imaging. The  $J_0$  Bessel nondiffracting transducer has an advantage that it does not require a diffraction correction when it is used for imaging. For relatively large homogeneous organs (such as human livers), once the attenuation of the tissue in the axial direction is properly compensated, short time FFTs can be applied to A-lines before they form a B-scan image. Sliding averages of the FFTs in the scanning (lateral) direction at the central frequency of the electrical tone bursts which excite the  $J_0$  Bessel nondiffracting transducer will form a backscatter coefficient image. The lateral resolution of the backscatter coefficient image will be determined by the length of the lateral sliding average while the axial resolution will depend upon the window width of the time gate used in short time FFTs. The larger the length of the lateral sliding average is, the smaller the standard deviation of the backscatter coefficients and the lower the lateral resolution will be. The larger the window width of the time gate is, the more accurate the estimation of the backscatter coefficients and the lower the axial resolution of the backscatter coefficient imaging will be.

### Side Lobes

The amplitudes of the sidelobes of the  $J_0$  Bessel nondiffracting transducer in pulse-echo imaging are determined by the square of the  $J_0$  Bessel function [13]. The sidelobes increase the size of the equivalent resolution cell in the lateral direction increasing the correlation between adjacent A-lines and decreasing the resolution in backscatter coefficient imaging. One way to solve the problem is to use Wiener filtering to reduce the sidelobes and hence to increase the lateral resolution prior to the processing to get the backscatter coefficient image. Because of the nonspreading character of the  $J_0$  Bessel beam, only a few kernels are required to perform two-dimensional Wiener filtering for the entire imaging region of interest.

### CONCLUSION

We describe a method for estimating backscatter coefficients of the excised human liver samples and the RMI413A tissue equivalent phantom, using the  $J_0$  Bessel nondiffracting transducer. These results compare well to those obtained by the conventional focused Gaussian beam

transducer for which the accuracy was verified by comparing to Faran's theory by other investigators [14].

The backscatter coefficients estimated by the  $J_0$  Bessel nondiffracting transducer are more distance independent than those estimated by the focused Gaussian beam transducer. This is due to the nonspreading nature of the  $J_0$  Bessel nondiffracting beam.

Because of the nonspreading nature of the  $J_0$  Bessel nondiffracting beam, signal processing for obtaining the backscatter coefficients is greatly simplified. This results in a tremendous reduction in computation time and creates the capability of calculating the backscatter coefficients in real time.

### ACKNOWLEDGMENTS

This work was supported in part by grant CA 43920 from the national Institutes of Health. The authors appreciated the help of Randall R. Kinnick for building the pulse-echo circuits of the nondiffracting transducer. The authors also appreciated the help given by Dr. Robert C. Bahn and Mr. Gerald E. McGrath in the Department of Pathology for making the human liver samples. The authors thank Mr. David J. Anders and Mr. Darrel T. Rowe of the Department of Imaging Maintenance for providing the RMI413A tissue equivalent phantom. The authors are grateful for the secretarial assistance of Elaine C. Quarve and graphical assistance of Christine A. Welch.

### REFERENCES

- [1] Durmin, J.: Exact solutions for nondiffracting beams. I. The scalar theory. *J. Opt. Soc. Am.* 4(4):651-654, 1987.
- [2] Durmin, J. and J. J. Miceli, Jr.: Diffraction-free beams. *Phys. Rev. Lett.* 58(15):1499-1501, 1987.
- [3] Durmin, J., J. J. Miceli, Jr., and J. H. Eberly: Experiments with nondiffracting needle beams. *Optical Society of America, Washington, DC, available from IEEE Service Center (87CH2391-1), Piscataway, NJ, 1987, p. 208.*
- [4] Gori, F., G. Guattari, and C. Padovani: Bessel-Gaussian beams. *Optics Commun.* 64(6):491-495, Dec 15, 1987.
- [5] Gori, F., G. Guattari, and C. Padovani: Model expansion for  $J_0$ -correlated Schell-model sources. *Optics Commun.* 64(4):311-316, Nov. 15, 1987.
- [6] Uehara, K. and H. Kikuchi: Generation of near diffraction-free laser beams. *Appl. Physics B* 48:125-129, 1989.
- [7] Vicari, L.: Truncation of nondiffracting beams. *Optics Commun.* 70(4):263-266, March 15, 1989.
- [8] Zahid, M. and M. S. Zubairy: Directionality of partially coherent Bessel-Gauss beams. *Optics Commun.* 70(5):361-364, April 1, 1989.
- [9] Cai, S. Y., A. Bhattacharjee and T. C. Marshall: 'Diffraction-free' optical beams in inverse free electron laser accelerators. *Nuclear Instruments and Methods in Physics Research, Section A: Accelerators, Spectrometers, Detectors and Associated Equipment* 272(1-2):481-484, Oct., 1988.
- [10] Hsu, D. K., F. J. Margetan, and D. O. Thompson: Bessel beam ultrasonic transducer: Fabrication method and experimental results. *Appl. Phys. Lett.* 55(20):2066-2068, Nov. 13, 1989.
- [11] Ziolkowski, R. W., D. K. Lewis, and B. D. Cook: Evidence of localized wave transmission. *Phys. Rev. Lett.* UME62(2):147-150, Jan. 8, 1989.
- [12] Lu, J.-y. and J. F. Greenleaf: Ultrasonic nondiffracting transducer for medical imaging. *IEEE Trans. UFFC.* 37(4):438-447, Sept., 1990.
- [13] Lu, J.-y. and J. F. Greenleaf: Pulse-echo imaging using a nondiffracting beam transducer. *Ultrasound Med. Biol.* (In Press).
- [14] Madsen, E. L., M. F. Insana, and J. A. Zagzebski: Method of data reduction for accurate determination of acoustic backscatter coefficients. *J. Acoust. Soc. Am.* 76(3):913-923, Sept., 1984.
- [15] Insana, M. F., E. L. Madsen, T. J. Hall, and J. A. Zagzebski: Tests of the accuracy of a data reduction method for determination of acoustic backscatter coefficients. *J. Acoust. Soc. Am.* 79(5):1230-1236, May, 1986.
- [16] Hall, T. J., E. L. Madsen, J. A. Zagzebski, and E. J. Boote: Accurate depth-independent determination of acoustic backscatter coefficients with focused transducers. *J. Acoust. Soc. Am.* 85(6):2410-2416, June, 1989.
- [17] Bamber, J. C. and C. R. Hill: Acoustic properties of normal and cancerous human liver—I. Dependence on pathological conditions. *Ultrasound Med. Biol.* 7:121-133, 1981.